

Anti-Hyperon Enhancement through Baryon Junction Loops

Stephen E. Vance^{1,2} and Miklos Gyulassy¹

¹ *Physics Department, Columbia University, 538 West 120th Street, New York, NY 10027*

² *Institute for Nuclear Theory, University of Washington, Box 351550, Seattle, WA 98195*

(July 12, 2018)

Abstract

The baryon junction exchange mechanism recently proposed to explain valence baryon number transport in nuclear collisions is extended to study midrapidity anti-hyperon production. Baryon junction-antijunction ($J\bar{J}$) loops are shown to enhance $\bar{\Lambda}, \bar{\Xi}, \bar{\Omega}$ as well as lead to long range rapidity correlations. Results are compared to recent WA97 $PbPb \rightarrow Y\bar{Y}X$ data.

25.75.-q,24.10.Lx

arXiv:nucl-th/9901009v1 6 Jan 1999

Striking nonlinear nuclear enhancements of multistrange hyperons and anti-hyperons have been recently reported for central $Pb + Pb$ collisions at incident momentum of 158A GeV [1–3]. For example, the midrapidity density of $\Xi^-(ssd)$ is claimed [3] to be enhanced by an order of magnitude relative to the linear $A^{1.0} \sim 200$ extrapolation from pp data. Multiparticle production models such as HIJING [4], FRITIOF [5], and DPM [6], which are based on the diquark-quark string picture for excited baryons, underestimate the midrapidity Λ yield by a factor of 6 (see [7]) and the Ω^- yield by a factor of 10^3 (see Figure 2). Recently, diquark breakup mechanisms have been proposed [8–11] that can account for at least part of the leading “valence” hyperon enhancements, but thus far none of those models have been able to account for the observed $\bar{\Lambda}, \bar{\Xi}, \bar{\Omega}$ enhancements.

Large hyperon and anti-hyperon enhancements are of particular interest since they have been proposed as one of the signatures of the quark-gluon plasma formation in nuclear collisions [12–14]. We argue that an equilibrated plasma interpretation of this data is problematic since chemical equilibration is slow and since adjustable fugacity parameters are needed to reproduce the anti-hyperon yields. In addition, still more parameterizations of the baryon chemical potential and transverse collective velocity fields are needed in order to fit the detailed rapidity and transverse momentum distributions of the hyperons and the anti-hyperons, which differ considerably.

Another non-equilibrium mechanism which mimics the effects of an equilibrated plasma by being able to enhance the strangeness yields is the fusion of strings into color “ropes” [15,16]. Increasing the string tension or energy density of the string increases greatly the Schwinger tunneling probability [17,18] of $s\bar{s}$ and $(ss)(\bar{s}\bar{s})$ production. However, the main drawback of the rope model is that the rope tension or string radius is unconstrained by pp and pA data and is taken as a free parameter to fit AA data. Ropes provide therefore the same freedom to fit data as fugacities, chemical potentials, and flow velocities in the above plasma fireball models.

In this letter, we propose instead a novel non-equilibrium hadronic mechanism derived from the Y-shaped ($SU_c(3)$) gluon structure of the baryon to explain these observations. In addition, this mechanism has the virtue that its parameters are in principal fixed by pp and pA phenomenology. In particular, we extend the valence baryon junction exchange mechanism in [10,19] by including junction-antijunction ($J\bar{J}$) loops that naturally arise in Regge phenomenology.

The concept of a baryon junction, $J(x)$, which links the three color flux (Wilson) lines flowing from the valence quarks, was developed in the context of Regge theory [19]. Several states, such as the quarkless hybrid glueball ($J\bar{J}$ or M_0^J) and hybrid exotic mesons [$(qJ\bar{J}\bar{q} = M_2^J)$ and $(qqJ\bar{J}\bar{q}\bar{q} = M_4^J)$], were proposed by linking junctions, anti-junctions and quarks in different ways. Historically [19], the M_0^J trajectory was invoked to explain the difference in multiplicities between the total inelastic cross sections of $p + \bar{p}$ and $p + p$ scattering. However, since the experimental results were not conclusive (due to the low energies involved) and since the M_i^J states have not been observed spectroscopically (presumably due to its large decay width), the junction concept lay dormant until recently.

A new test of the junction picture of the baryons was proposed in [10] based on an analysis of the valence ($p - \bar{p}$) rapidity distributions in high energy reactions. This baryon junction exchange mechanism for the flow of the baryon number was implemented in the HIJING/B event generator in [11]. It was shown to provide not only a very effective mechanism for the

transport of *valence* baryon number over a large rapidity intervals in nuclear collisions as observed in [20], but it also was shown to naturally enhance the “valence” hyperon ($Y - \bar{Y}$) production. However, as shown below, this diquark breakup mechanism is unable to explain the observed anti-hyperon enhancement.

The M_0^J or $J\bar{J}$ trajectory corresponds in operator form to the exchange of a closed three string configuration (three sheet topology) written below,

$$M_0^J = \epsilon^{j_1 j_2 j_3} \epsilon_{k_1 k_2 k_3} \left[P \exp \left(ig \int_{x_{\bar{j}}}^{x_j} dx^\mu A_\mu \right) \right]_{j_1}^{k_1} \left[P \exp \left(ig \int_{x_{\bar{j}}}^{x_j} dx^\mu A_\mu \right) \right]_{j_2}^{k_2} \\ \times \left[P \exp \left(ig \int_{x_{\bar{j}}}^{x_j} dx^\mu A_\mu \right) \right]_{j_3}^{k_3} . \quad (1)$$

When in a highly excited state, this $J\bar{J}$ three string configuration fragments into a baryon and an antibaryon with approximately three times the rapidity density of mesons of e^+e^- between the baryon pair. The fragmentation of the three independent strings naturally enhances the transverse momentum as well as the strangeness content of the baryon and the anti-baryon. In particular, the fragmentation of $J\bar{J}$ into Ω^- and $\bar{\Omega}^+$ is possible. In addition, novel long range rapidity correlations are predicted by this mechanism as shown below.

The generalized optical theorem and Regge theory [21] provide the calculus to compute the differential inclusive cross section of baryons resulting from $J\bar{J}$ exchange. The Regge diagram shown in Fig 1a represents the extra contribution to the single inclusive “valence” baryon distribution due to the junction exchange [10,21] and gives

$$E_B \frac{d^3\sigma}{d^3\mathbf{p}_B} \rightarrow C_B e^{-(\alpha_{M_0^J}(0)-1)y_B} , \quad (2)$$

where C_B is an unknown function of the transverse momentum of the “valence” baryon and the couplings of the M_0^J Regge state to the Pomeron and the baryons. Another diagram (same as Fig 1a, but where the P and the M_0^J are interchanged) gives rise to the contribution of $\exp((\alpha_{M_0^J}(0) - 1)y_B)$ for the target region. The contribution to the double differential inclusive cross section for the inclusive production of a baryon and an anti-baryon in NN collisions due to $J\bar{J}$ exchange (shown diagrammatically in Fig 1b) is

$$E_B E_{\bar{B}} \frac{d^6\sigma}{d^3\mathbf{p}_B d^3\mathbf{p}_{\bar{B}}} \rightarrow C_{B\bar{B}} e^{(\alpha_{M_0^J}(0)-1)|y_B - y_{\bar{B}}|} , \quad (3)$$

where $C_{B\bar{B}}$ is an unknown function of the transverse momentum and the $M_0^J + P + B$ couplings. We include these processes in the string model by introducing diquark breaking (Fig. 1c) and $J\bar{J}$ loop (Fig.1d) string configurations.

From Eq. (3), the predicted rapidity correlation length $(1 - \alpha_{M_0^J}(0))^{-1}$ depends upon the value of the intercept $\alpha_{M_0^J}(0)$. As in [11], we assume $\alpha_{M_0^J}(0) \simeq 1/2$. Our choice is based upon arguments and estimates from a multiperipheral model approximation [19,22] and is consistent with the multiplicity and energy dependence of $\Delta\sigma = \sigma_{p\bar{p}} - \sigma_{pp}$ [23]. This value $\alpha_{M_0^J}(0)$ can now again be tested through the rapidity correlations. To test for this M_0^J component ($\alpha_{M_0^J}(0) \simeq 1/2$) requires the measurement of rapidity correlations on a scale

$|y_B - y_{\bar{B}}| \sim 2$. We note that it would be especially useful to look for this correlation in high energy $p + p \rightarrow B + \bar{B} + X$, especially at RHIC where very high statistics multiparticle data will soon be available.

Replacing the M_0^J reggeon in Fig 3b with the Pomeron or other Reggeon states gives the remaining contributions to the double inclusive differential cross section. Replacing the M_0^J with the Pomeron leads to a uniform rapidity distribution which corresponds to the uncorrelated product of two single inclusive differential cross sections [21]. (The short range $\Delta y \sim 1$ dynamical (Schwinger) correlations in string models lie outside the Regge kinematic region). Replacing the M_0^J with other Reggeons such as the ω provides a contribution which is similar to Eq. (3) but with a different coupling and with $\alpha_R(0)$ instead of $\alpha_{M_0^J}(0)$. We argue that the contributions from these Reggeons is small since the contribution from the M_0^J seems to dominate the contribution from the ω in pp and $p\bar{p}$ scattering (see [19,23] and references therein). In addition, in the string picture, the contribution of the ω is modeled as single string between the baryon and the antibaryon which leads to lower multiplicities and does *not* provide a strangeness enhancement.

We modified HIJING/B [11] to include the above $J\bar{J}$ loops and the new version, called HIJING/B \bar{B} , is available at [24]. By fitting \bar{p} and $\bar{\Lambda}$ data from $p + p$ [25] and $p + S$ [26,27] interactions at 400 GeV/c and 200 GeV/c incident momentum, respectively, the cross section for $J\bar{J}$ exchange is found to be $\sigma_{B\bar{B}} = 6$ mb. We took the threshold cutoff mass of Fig. 1d configurations to be $m_c = 6$ GeV. This large minimum cutoff is necessary in order to provide sufficient kinematical phase space for fragmentation of the strings and for $B\bar{B}$ production. In addition, the applicability of the Regge analysis also requires a high mass between all of the external lines in Fig 1b. At SPS energies ($\sqrt{s} \sim 20$), this kinematic constraint severely limits the number of $J\bar{J}$ configurations allowed, reducing its effective cross section to ~ 3 mb. The \vec{p}_T of the baryons from the $J\bar{J}$ loops are obtained by adding the \vec{p}_T of the three sea quarks along with an additional soft p_T kick. The soft p_T kick is taken from a Gaussian distribution whose width $\sigma = 0.6$ GeV/c is fit to $p + S$ data [26] at 200 GeV/c. At collider energies, hard pQCD processes are modeled as kinks in strings as in HIJING [4].

In multiple collisions, a (color 6) diquark broken through a junction exchange in a previous collision has a finite probability to reform (color $\bar{3}$) in a subsequent collision. However, in the present implementation, we assume that when a junction loop is formed in a previous collision, then it cannot be destroyed in subsequent collisions. The pA data are consistent with these assumptions. We emphasize that the present version of HIJING/B \bar{B} does not include final state interactions. Although final state interactions such as (e.g. $N + \pi \rightarrow \Lambda + K$) and $Y + \bar{p} \rightarrow X$ can change the flavor and relative yields of many hadrons, we note that these interactions cannot easily enhance the multiplicities of the multi-strange baryons, Ξ and Ω .

In Figure 2, we show the computed net hyperon yields ($Y + \bar{Y}$) from the HIJING, HIJING/B and HIJING/B \bar{B} event generators for $p + Pb$, $S + S$ and $Pb + Pb$ at 160 AGeV. HIJING (open triangle) is seen to underpredict the hyperons in $Pb + Pb$ reactions. HIJING/B results (open squares) show that the valence junction exchange significantly enhances the multiple strange baryon yields. The anomalously large WA97 Ω yield (solid triangle) in $PbPb$ is not explained however. The $J\bar{J}$ mechanism in HIJING/B \bar{B} enhances the net ($Y + \bar{Y}$) yield only modestly. However, Figure 3 shows the large effect of the $J\bar{J}$ loops on the ratio of the yields of the antihyperons to the hyperons, $\eta = N_B/N_{\bar{B}}$. In HIJING, this ratio is close to 1 for

$S = -2, -3$ baryons because they are mostly formed via diquark-anti-diquark fragmentation of single strings. In HIJING/B, the splitting of the string in Figure 1c into three smaller mass strings strongly reduces the phase space for antihyperon production and leads to a very small ratio of η shown in Fig. 3. HIJING/ $B\bar{B}$ solves this problem by providing a natural channel that enhances anti-hyperons production.

Returning to the striking enhancement of the Ω in Figure 2, we note that the diamonds show that even a very modest rope enhancement of $\kappa = 1.4$ GeV/fm is enough to enhance the Ω by another factor of 10. This rare observable is exponentially sensitive to uncertainties in the multiparticle phenomenology. We note for example that there exist more complex multibaryon loop diagrams of junction - anti-junction vertices that can further enhance $\Omega\bar{\Omega}$ production. We do not pursue such possibilities here, but leave them for another work, since our main point here is to show that $J\bar{J}$ loops are natural and provide a qualitative explanation of the observed moderate antihyperon/hyperon ratios in Fig.3.

Finally, we predict in Fig. 4 the initial distribution of antibaryons for $Au + Au$ collisions at $\sqrt{s} = 200A$ GeV for $b \leq 3$ fm. The estimates for the \bar{p} in HIJING/ $B\bar{B}$ are a factor of 3 lower than the original HIJING prediction. This results from correcting for an overpredicted (factor of 2) \bar{p} yield by HIJING for $p + p$ collisions at 400 GeV/c and allowing at most one $J\bar{J}$ loop in the wounded nucleon string. The $\bar{\Lambda}$ are less effected (factor of 2.5) by these corrections due to the extra strangeness enhancement from the fragmentation of the $J\bar{J}$ loops.

In summary, we showed that modifications in the multiparticle production dynamics which are consistent with pp and pA physics can yield significant (anti)hyperon production as well baryon stopping power in AA collisions. The large WA97 antihyperon/hyperon yields require $J\bar{J}$ loops in this approach. However, the absolute yields of especially the $\Omega^-(sss)$ are still underestimated (without ropes or more complex multibaryon junction diagrams). Upcoming measurements at RHIC on baryon number transport and $B\bar{B}$ correlations will be especially important in clarifying whether indeed the $J\bar{J}$ exchange mechanism plays a dominant role in hyperon dynamics.

This work was supported by the Director, Office of Energy Research, Division of Nuclear Physics of the Office of High Energy and Nuclear Physics of the U.S. Department of Energy under Contract No. DE-FG02-93ER40764. S.E. Vance also thanks the Institute for Nuclear Theory at the University of Washington for its hospitality during which part of this project was completed.

REFERENCES

- [1] E. Andersen, et al., (WA97 Collaboration), Phys. Lett. **B433** (1998) 209.
- [2] S. Margetis et al., (NA49 Collaboration), Proceedings of the Conference on Strangeness in Hadronic Matter, Strangeness '98.
- [3] H. Appelshäuser, et al., (NA49 Collaboration), nucl-ex/9810005.
- [4] X. N. Wang and M. Gyulassy, Phys. Rev. **D44** (1991) 3501; Phys. Rev. **D45** (1992) 844; Comp. Phys. Comm. **83** (1994) 307 .
- [5] B. Andersson, et al., Nucl. Phys. **B281** (1987) 289; Comp. Phys. Commun. **43** (1987) 387.
- [6] A. Capella, U. Sukhatme, C. I. Tan and J. Tran Thanh Van, Phys. Rep. **236** (1994) 225.
- [7] V. Topor Pop, et al., Phys. Rev. **C52** (1995) 1618; M. Gyulassy, V. Topor Pop, X. N. Wang, Phys. Rev. **C54** (1996) 1497.
- [8] B.Z. Kopeliovich and B.G. Zakharov, Z. Phys. C, **43**, (1989) 241.
- [9] A. Capella, B.Z. Kopeliovich, Phys. Lett. **B381** (1996) 325; hep-ph/9603279.
- [10] D. Kharzeev, Phys. Lett. **B378** (1996) 238, nucl-th/9602027.
- [11] S.E. Vance, M. Gyulassy and X.N. Wang, Phys. Lett **B**, in press, nucl-th/9806008.
- [12] J. Rafelski, Phys. Rep. **88** (1982) 311.
- [13] J. Rafelski and B. Müller, Phys. Rev. Lett. **48** (1982) 1066.
- [14] P. Koch, B. Müller, and J. Rafelski, Phys. Rep. **142** (1986) 167.
- [15] T.S. Biro, H.B. Nielsen, and J. Knoll, Nucl. Phys. **B245** (1984) 449.
- [16] H. Sorge, Phys. Rev. **C52** (1995) 3291; nucl-th/9509007.
- [17] J. Schwinger, Phys. Rev. **82** 664 (1951).
- [18] B. Andersson, G. Gustafson, G. Ingelman, T. Sjostrand, Phys. Rept. **97** (1983) 31.
- [19] G.C. Rossi and G. Veneziano, Nucl. Phys. **B123** (1977) 507; Phys. Rep. **63** (1980) 153.
- [20] H. Appelshäuser, et al., (NA49 Collaboration), submitted to Phys. Rev. Lett., nucl-ex/9810014.
- [21] P.D.B. Collins, "An Introduction to Regge Theory and High Energy Physics", Cambridge University Press, Cambridge, © 1977.
- [22] Y. Eylon and H. Harari, Nucl. Phys. **B80** (1974) 349.
- [23] S.E. Vance, V. Topor Pop and M. Gyulassy, in preparation.
- [24] see <http://www-cunuke.phys.columbia.edu/people/svance/hjbb.html>
- [25] M. Aguilar-Benitez et al. (LEBC-EHS Collaboration), Z. Phys. **C50** (1991) 405.
- [26] T. Alber et. al., (NA35 Collaboration), Z. Phys. **C64** (1994) 195.
- [27] T. Alber et. al., (NA35 Collaboration), Eur. Phys. J. **C2** (1998) 643.

FIGURES

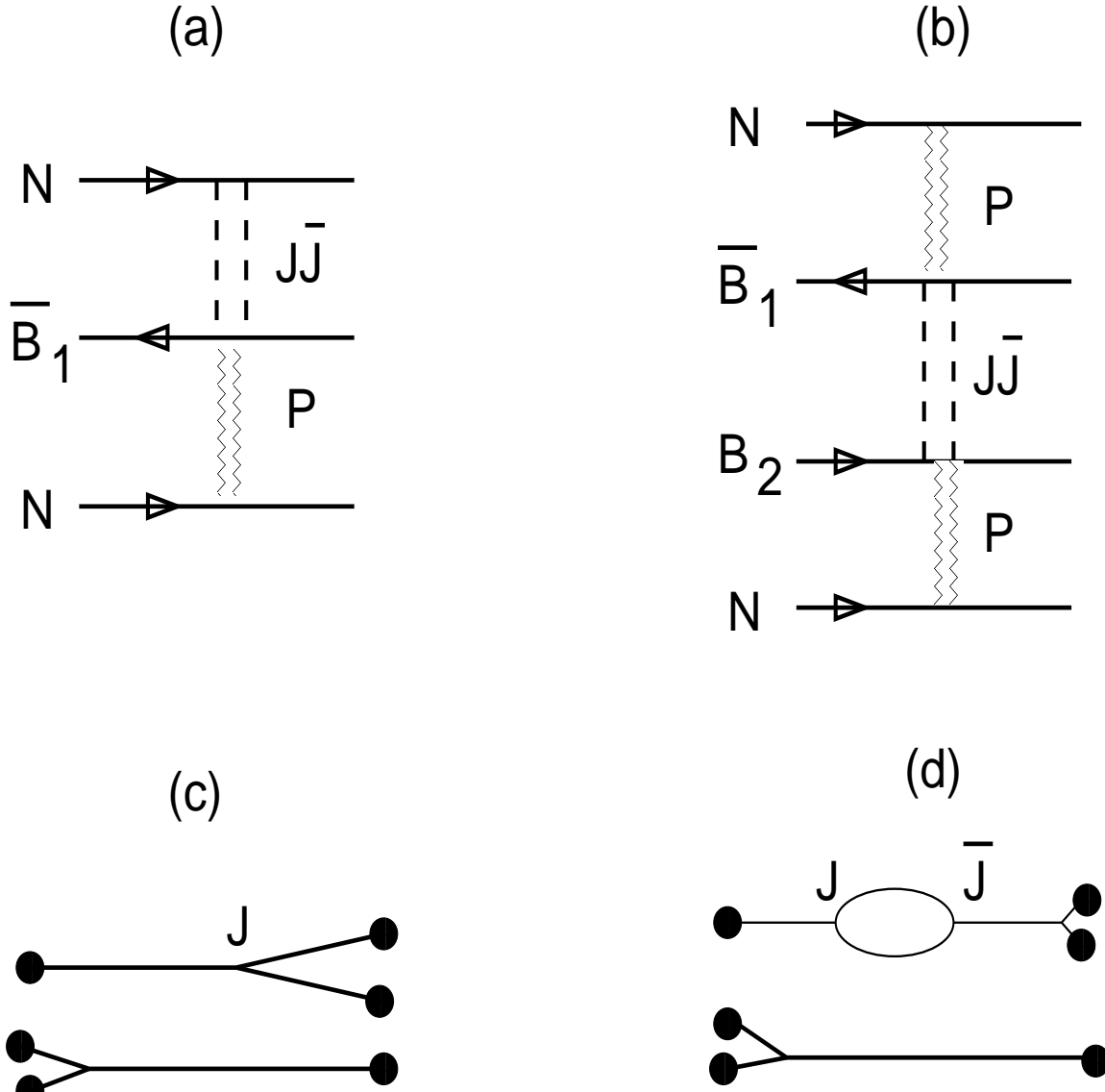


FIG. 1. The Regge diagrams for the single baryon junction exchange and $J\bar{J}$ loops are shown in (a) and (b), respectively. The string model implementation of each Regge diagram are shown in (c) and (d).

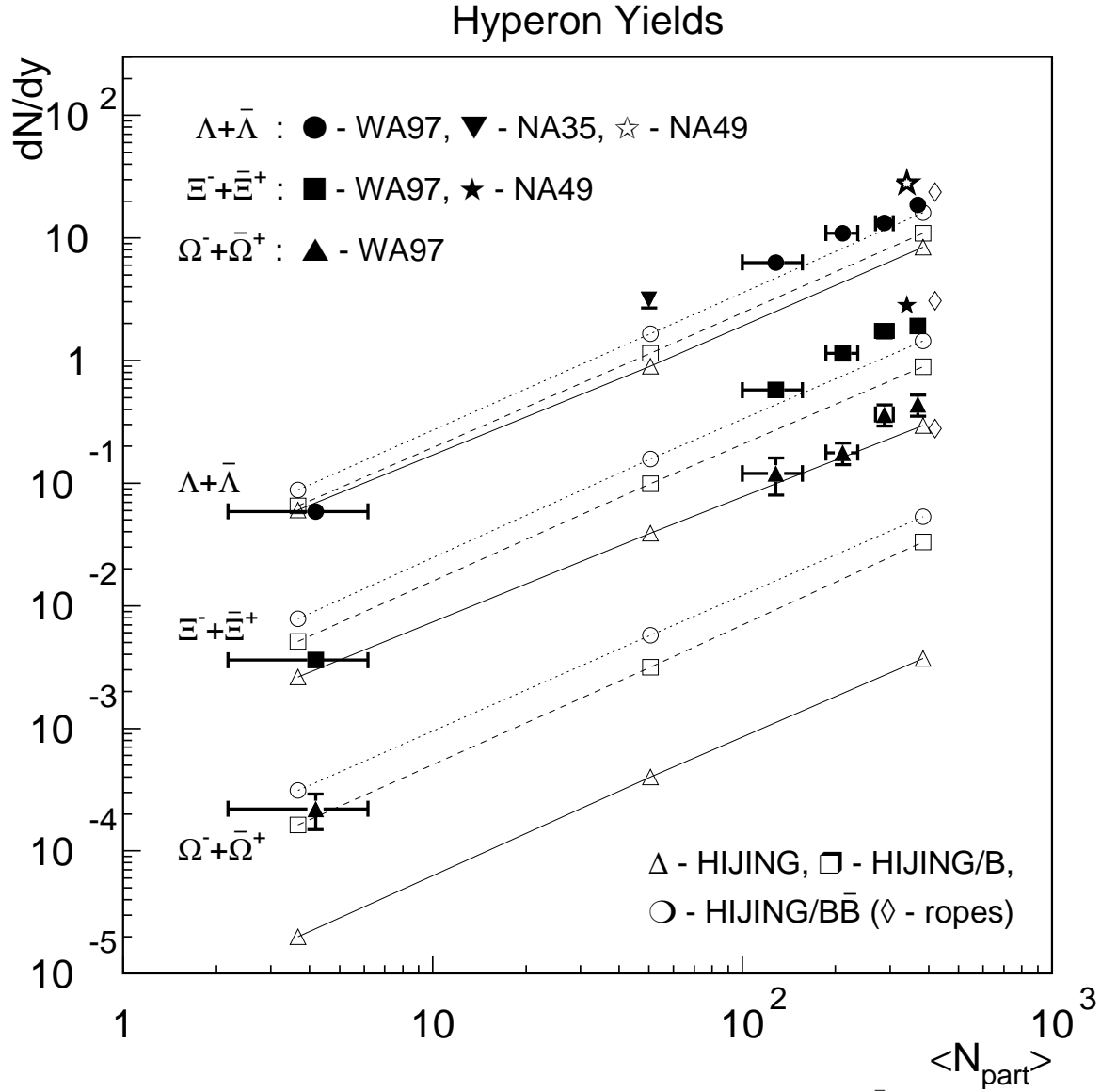


FIG. 2. Hyperon yields from HIJING, HIJING/B and HIJING/B \bar{B} for $p + Pb$, $S + S$ and $Pb + Pb$ at incident momentum $p_{lab} = 160$ AGeV are shown along with data from the NA35 [26], the NA49 [2,3] and the WA97 [1] collaborations.

Hyperon Ratios

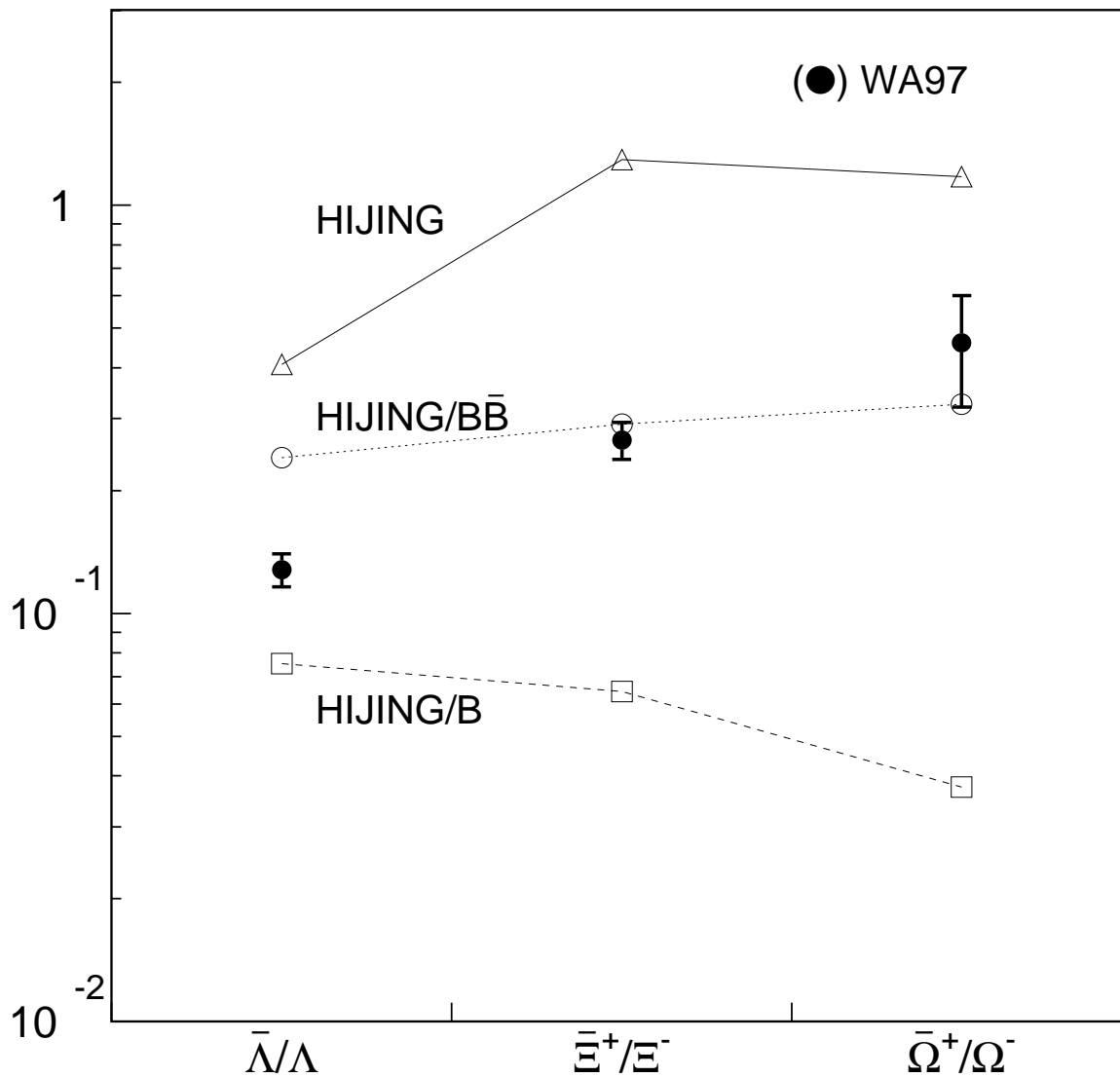


FIG. 3. The ratios of the yields of antihyperons to hyperons are shown for HIJING, HIJING/B and HIJING/ $B\bar{B}$ for $p + Pb$, $S + S$ and $Pb + Pb$ at incident momentum $p_{lab} = 160$ AGeV along with data from the WA97 [1] collaboration.

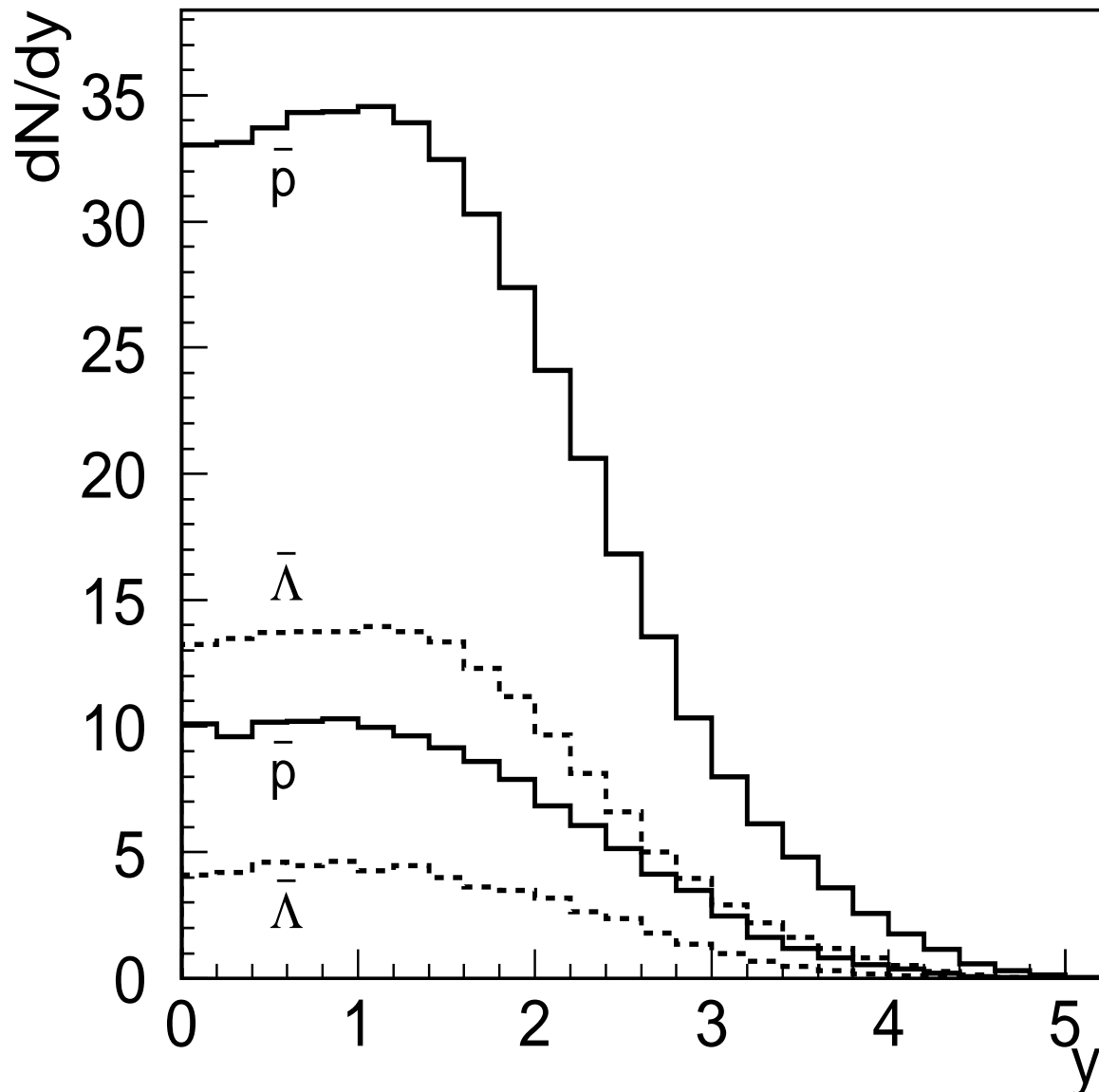


FIG. 4. Predictions for the initial \bar{p} (solid lines) and $\bar{\Lambda}$ (dashed lines) rapidity distributions are given for HIJING (upper solid and dashed curves) and for HIJING/ $\bar{B}\bar{B}$ (lower solid and dashed curves) for Au+Au collisions at $E_{cm} = 200$ at $b \leq 3$ fm.